FOC Objective Prisms: Calibrations and Software

W. Hack
April 19, 1996

ABSTRACT

A new set of F/96 near-UV (NUVOP) and far-UV (FUVOP) dispersion curves have been derived based on Cycle 4 calibration observations of an emission line source and a spectrophotometric standard. These dispersion curves provide photometry with errors of approximately 0.1 magnitudes from 1600-4000Å for the NUVOP and 1200-3000Å for the FUVOP. Furthermore, the dispersion curves have rms errors in the fit of 3.4 pixels for the NUVOP and 0.87 pixels for the FUVOP. These errors in the fit correspond to errors in wavelength determination of 1.8Å at 1600Å and 17Å at 2500Å with the NUVOP and 1.3Å at 1200Å and 16Å at 1800Å in the FUVOP. In addition to improved calibrations, the techniques and software for reducing objective prism data (and used in producing the dispersion curves) are outlined using the calibration observations as an example. As a result, observers should be able to follow the procedures described here and use the dispersion curves provided to reduce objective prism data.

1. Introduction

The objective prisms have been difficult to calibrate due to the difficulty in finding suitable emission line sources. In previous cycles, V1329 Cyg served as the initial calibration source exhibiting 5 emission lines which were used to provide the initial calibration for each of the prisms. This initial calibration was reported in the FOC SV report. However, the dispersion curves still showed differences in the photometry of 20% or more when compared to simulations of spectrophotometric standards. It was these errors that were addressed in the Cycle 4 calibration efforts.

Observations were made in Cycle 4 of another emission line object for which IUE spectra had been independently obtained: Sanduleak 3, a high-excitation Wolf-Rayet star. This report describes the observations taken of this new ‘standard’ and of HZ4 (a spectrophotometric standard for HST). The larger number of emission lines present in these new observations allowed for the derivation of a dispersion curve which is accurate over nearly

the entire wavelength region observed by the FOC. This report will discuss the new curves, along with the level of accuracy that can be expected, both in wavelength determinations and in the spectrophotometry.

This report also provides the details for reducing objective prism images to produce flux-calibrated spectra using the new dispersion curves. Included in the discussion will be sections describing a number of factors which can result in errors in reducing these images, including filter shifts and extraction of the spectra from the image.

2. Observations

Objective prism images of Sand-3 were taken in Cycle 3 with the objective of obtaining a calibration source presenting emission lines over a wider wavelength range than V1329 Cyg. These observations proved that this target displays many emission lines all throughout the spectrum. Unfortunately, the spherical aberration and small imaging format made analysis of the data difficult. The observations were repeated with the COSTAR-corrected FOC in the Cycle 4 proposal 5740 using the 256 x 1024 format. These observations obtained the entire near-UV objective prism spectrum as well as the position of the star without the prisms in place. However, Sand-3 has not been established as a photometric standard, so observations with the objective prism were included in the Cycle 4 proposal 5517. These additional observations of a spectrophotometric standard served as a final test of the objective prisms' photometric calibration.

The wavelength calibration proposal (Prop. 5740) was executed on 31 Aug 1994 starting with a 512z x 1024 (X96ZLRG) format INT ACQ image to properly center the target in the field of view for use of the narrow 256 x 1024 (X96NREC) format. The full set of images taken in this proposal are described in Table 1. Basically, a direct image and a prism image were taken at the same POS TARG position for each prism, so that an unambiguous determination of the offset induced by the prisms can be directly measured from the position of the star in the direct image. The only source of error remaining in determining the offsets comes from the uncertainty in the filter shifts. These shifts move the position of the star in the image, and since the direct images use different filters from the prism images, it results in different relative positions between the star and the position of features in the spectrum, i.e. the offset of the feature.

Table 1. Exposure log for Proposal 5740 (wavelength calibration) and prism images from Proposal 5517 (photometric calibration).

Rootname	PHOTMODE	Exp. Time	Comments
Proposal 5740 - Sand-3 observations			
x2hv0101	F210M,F4ND,X96ZLRG	600.	INT ACQ image
x2hv0102	F210M,F4ND	600.	Undispersed image for FUV spectra

Rootname	PHOTMODE	Exp. Time	Comments
x2hv0103	PRISM1,F140W,F1ND	736.	FUV prism image
x2hv0104	F501N,F2ND	600.	Undispersed image for NUV spectra
x2hv0105	PRISM2,F175W,F1ND	900.	NUV + F175W prism image
x2hv0106	PRISM2,F165W	900	NUV + F165W prism image
	Proposal 5517 - HZ4 observations		
x2ap020d	F501N,F2ND,X92NREC	300	Direct image at same position as NUV images POS TARG of 0,-2”
x2ap020e	PRISM2,F175W	900	NUV + F175W prism image
x2ap020f	PRISM2,F195W	600	1st part of NUV + F195W prism image
x2ap020g	PRISM2,F195W	300	2nd part of NUV + F195W prism image
x2ap020h	PRISM2,F275W,F195W	900	NUV + F195W + F275W prism image
x2ap020i	PRISM1,F140W	665	1st part of FUV + F140W prism image POS TARG of 0,-4”:
x2ap020j	PRISM1, F140W	225	2nd part of FUV+F140W prism image POS TARG of 0,-4”
x2ap020k	PRISM1,F140W,F130LP	900	FUV + F140W + F130LP prism image POS TARG of 0,-4”

High S/N images were obtained, with each direct image having peak values of 101 counts (0.16 counts sec^{-1} pix^{-1}) for the F210M image and 516 counts (0.87 counts sec^{-1} pix^{-1}) for the F501N image. These linear images allowed for easy determination of the star’s position using *imcntr* or even *minmax*. The prism images had equally high S/N, as seen qualitatively in Figure 1. The FUV spectrum had a peak count rate of 0.75 counts sec^{-1} pix^{-1} for the C IV 1550Å line, while count rates of 0.25 and 1.11 counts sec^{-1} pix^{-1} were measured for the Mg II emission line in the F175W NUV and F165W NUV spectrum, respectively. The continuum, on the other hand, remained at count rates below 0.25 counts sec^{-1} pix^{-1} throughout all images.

Objective prism images turn point sources into extended sources, being an extended source in the dispersion (Y) direction and a point source in the spatial (X) direction. As a result, they had linearity characteristics which fall between those of a point source and of an extended source. The continuum count rates in the calibration images were only modestly above the 0.15 counts sec^{-1} pix^{-1} for 10% non-linearity for an extended source, and therefore did not suffer from significant non-linearity.

The observations of HZ4 (the spectrophotometric standard) listed in Table 1 were taken on 27 Mar 1994. They consisted of a direct image taken with the F501N filter at a POS TARG of (0,-2”), the same target position as the NUV prism images were taken at, while the FUV prism images were taken at a POS TARG of (0,-4”). These images were equally well

exposed, with only low-levels of non-linearity (~10%) in the visible end NUV + F195W spectra.

A complication arose in the fact that the format used (256 x 1024) did not originally have a geometric correction file, i.e. it could not be geometrically corrected. Cycle 4 calibrations were undertaken to provide improved geometric distortion corrections using a new method, and this format was subsequently calibrated (see FOC-087 for more details). The geometric correction for this format was then applied individually to the prism calibration images prior to any final reductions or analysis. These new geometric correction files were designed to allow for proper registration between images taken in different formats making the prism calibrations derived from one format to be equally applicable to spectra taken in other formats (i.e., the 512 x 512 format).

Figure 1: a) Near-UV (NUV+F165W) and **b)** far-UV (FUV+F140W) objective prism images of Sand-3. The images were normalized to the same exposure time and are shown using the same linear contrast scale.

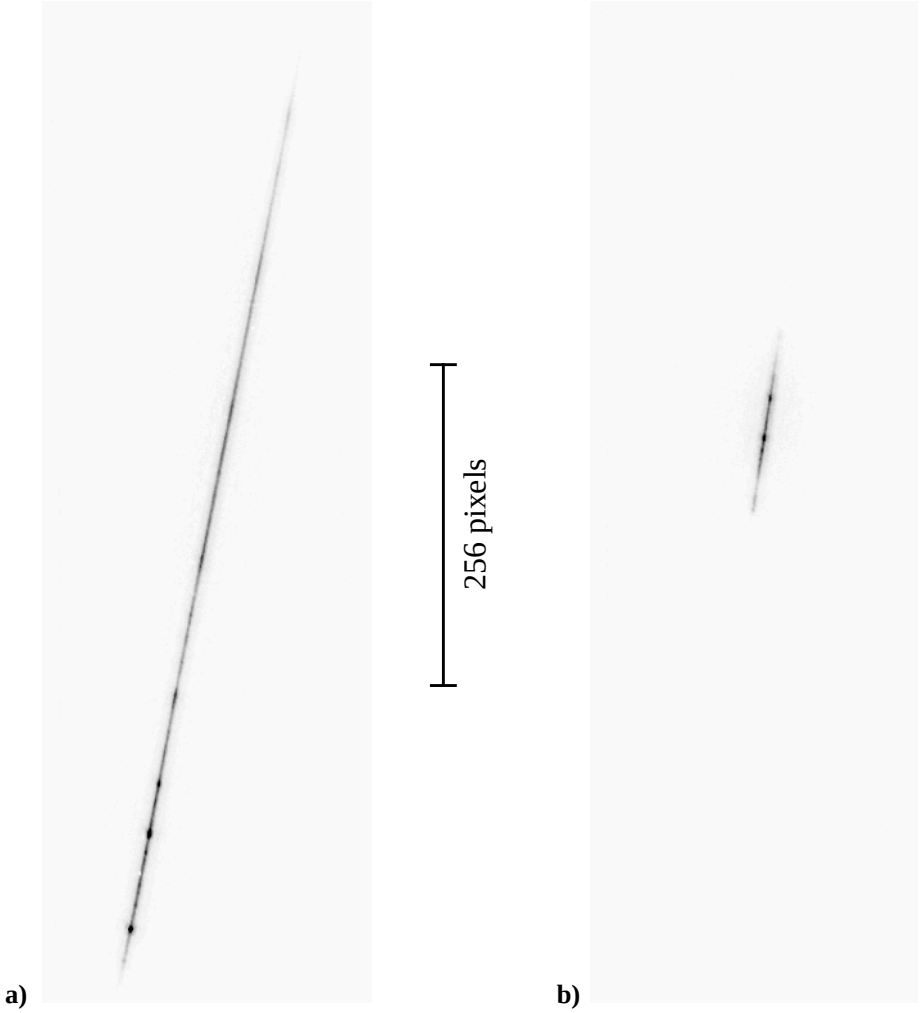

3. Reduction Technique and Software

A technique for extracting the spectrum from an objective prism image and applying the wavelength and flux calibrations was refined to take advantage of available IRAF software and the specialized software written for the prisms. This allowed the dispersion curves to be derived using the same method with which an observer would extract the spectrum from the background-subtracted image, providing consistency in the application of the calibrations. The general steps for this reduction are to:

1. extract the raw spectrum,
2. determine the position of the undispersed image,
3. calculate the percent of light contained in the extracted spectrum, and finally
4. wavelength and photometrically calibrate the raw spectrum.

The result of applying this technique would be a flux-calibrated, wavelength corrected spectrum in units of ergs cm^{-2} sec^{-1} $Å^{-1}$. These steps, although fairly basic, still require some care in order to assure proper calibration of the raw spectrum. The specific operations for each step is described in the following sections using the calibration observations of Sand-3 as an example of the calibration process.

Extraction of the Spectrum

The angle that the objective prism spectrum makes across an FOC image precludes the use of simple row or column based extraction methods without re-sampling the image through rotation. Any re-sampling due to rotation of the image, however, would introduce uncertainty into the determination of the zero-point of the calibrations, and stretch the spectrum over more pixels in the Y-direction. A two dimensional extraction avoids these pitfalls providing a simpler reduction.The method chosen for the calibrations was the *apall* extraction from the *noao.twodspec.apextract* package under IRAF. This task has the advantage of being interactive in its application to the image, and suitable for extracting multiple spectra from a single image (as would be the case for a prism image of a field of stars).

The steps for using the *apall* task are similar to almost any IRAF task. For the extraction of a spectrum from an FOC image, the following steps were used:

- the command *epar apall* was used to bring up a listing of all the necessary parameters for starting the task.
- the image name was given for the parameter *input* and a filename was provided for the output file in the parameter *output*
- the parameter *interactive* was set to ‘yes’ and the rest of the parameters were left at the default values to be changed while running the task
- the command :go was used to start the task

The task then displayed a plot of the central row of the image, at Y=512 in the 256x1024 image, which showed a cross-section of the spectra in the image. Above the peak that represents the spectrum, a bar is displayed showing the upper and lower limits of the extraction aperture.

The 7-pixel wide extraction was set using the commands:

- *:lower -3.5* set the lower limit to -3.5 pixels from the core of the spectrum, then
- *:upper 3.5* set the upper limit to 3.5 pixels from the core.

This display was exited by typing *q*, and a fit was automatically made along the core of the spectrum in the image. The points it found along the spectrum are then displayed in a plot shown in Figure 2 for the NUVOP+F165W image of Sand-3 (`x2hv0106`). The fit was cleaned up with the following steps:

- those points originating outside the spectrum were deleted by placing the cursor on them and typing ‘d’, putting an X on them as shown in Figure 2.
- a new fit was made by typing ‘f’.
- once the fit is completed, the extracted spectrum will be displayed and typing *q* will exit the task.

Once the fit was made, the 7 pixel wide extraction was performed along the fit and output to a 1-D image, which is displayed in Figure 3 for the extraction shown in Figure 2.

Figure 2: Fit along the NUVOP+F165W spectrum of Sand-3 as made using the apall task. The fit is shown as the dashed line while the extraneous points, from outside the spectrum on the image, that were deleted are shown with an 'X'.

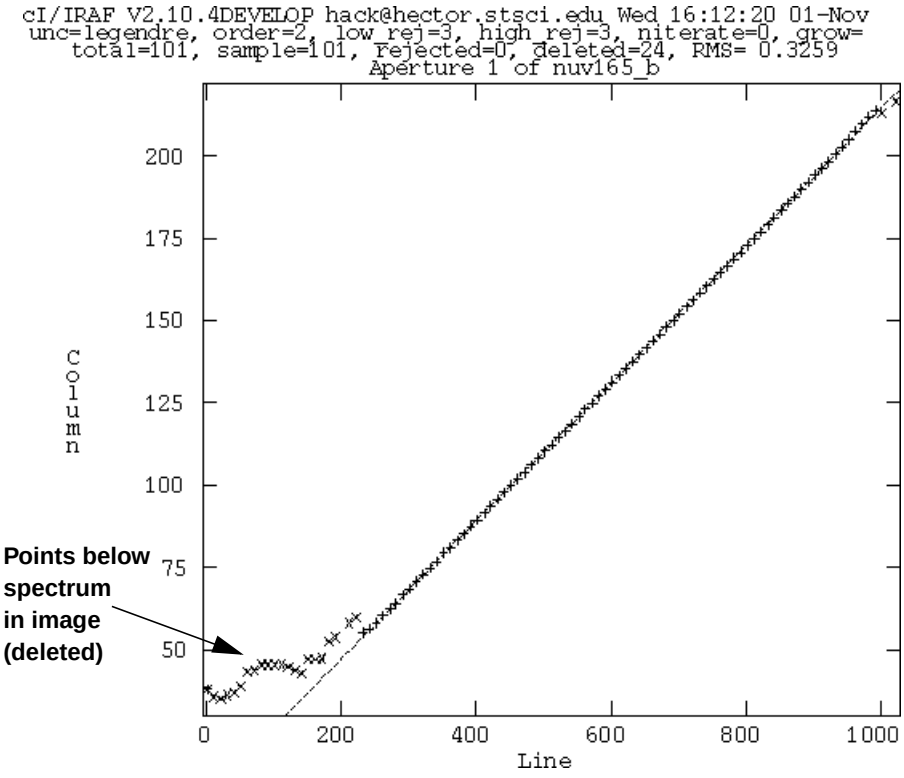

The width of the extraction can be varied depending on the signal in the spectrum and on whether it is an individual spectrum in the image or one of many, with narrower extractions being used on sources in crowded fields to limit contamination by nearby sources. Multiple spectra can be extracted into the same output image by marking all the desired spectra in the plot of a row from the image, then by fitting each spectrum individually; see the on-line help in *apall* for more details on how this can be done.

Figure 3: Plot of the 7-pixel wide extraction from the NUVOP+F165W spectrum of Sand-3. A number of the major lines used in the calibration are identified on the spectrum.

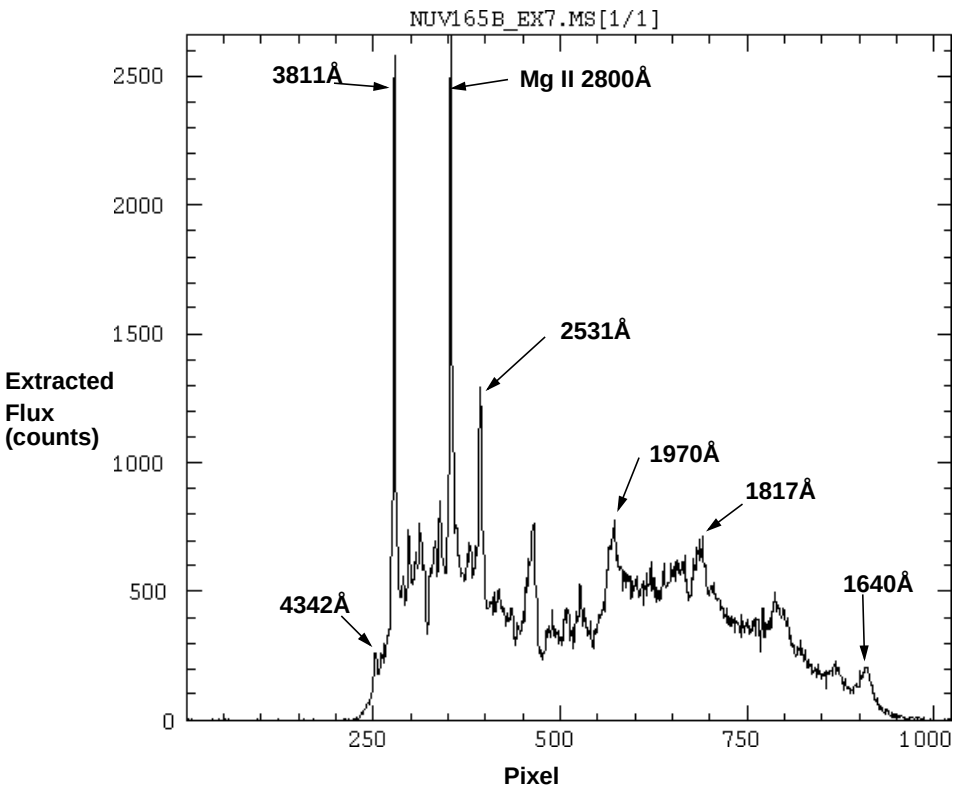

Position of the Undispersed Image

Application of the dispersion curve to the spectrum relies on knowing where the undispersed image was when the prism was in place in order to assign wavelengths along the observed spectrum. There are three distinct ways to obtain the undispersed position of the source:

- observing the target with the same POS TARG without the prisms
- assigning a wavelength to a known line/feature in the observed spectrum, or
- measuring the red end of the spectrum.

As a rule, at least 1 of these methods can be applied to any given image, and often all three can be measured, providing a consistency check on the zero-point determination for the calibrations. This is especially important for those programs which may not have all the information necessary for one method, such as programs without direct images of the target at all.

Direct Image comparison

The position of the target in an image taken at the same POS TARG as the prism image provides the most direct and unambiguous determination of this value. This is especially important for sources which have high radial velocities or which have lines at unknown velocities. In both of these cases, the actual wavelength of the line is not known and can not be used for determining the target's undispersed position (as described in the following section), and only the direct image can provide this information. For the Sand-3 images (which has broad emission lines), an image taken with only the F501N+F2ND (`x2hv0104`) was taken at the same POS TARG position in the same format as the following NUVOP observations. The pixel position of the star in the geometrically corrected image was Y=392, corresponding to the value needed for the analysis.

Spectral Feature Identification

Without a direct image, features in the prism image can be used to determine this zero-point. The wavelength of an identifiable emission line can be looked up in the prism dispersion table. These tables are available in the *focprism* directory as *f96_fuv_disp.dat* for the F/96 far-UV prism and *f96_nuv_disp.dat* for the F/96 near-UV prism. This wavelength should be known for this particular target, either from calibrated spectra from other sources (e.g., FOS or IUE) or from emission line tables assuming the source has little or no significant radial velocity. The associated offset for that line can then be added to the Y position of the line in the spectrum to obtain the undispersed position of the target. For example, the 2531Å C IV+ O VII line can be identified in a NUV spectrum of Sand-3 at Y=393. The offset for 2531Å from the NUV dispersion curve is -1 pixel, meaning the undispersed image was at Y= 392, corroborating the position determined directly from the F501N image.

Errors in this determination can arise from image shifts induced by the filters used in combination with the prisms, for the direct images, or both. The position of the target in the direct image can be shifted by the filters and cause the dispersion curve to be applied incorrectly. These errors can be as large as 17 pixels (0.24"). This translates to ~17 Å at 1200Å and ~300Å at 1800Å with the FUVOP, and ~17 Å at 1800Å and ~200Å at 3100Å with the NUVOP. The known filter shifts for F/96 filters can be found on the FOC WWW pages in the Calibration Products and Tools page. None of the direct images taken for these calibrations used a filter which had any filter shift in the Y direction, however, the F140W filter used with some of the FUV prism images has a 2 pixel shift in Y. For the Sand-3 images, the undispersed image was at Y= 392 for the NUV prism images and at Y=249 for the FUV prism images, but correcting for the filter shift of the F140W filter resulted in Y=251 being used. Fortunately, this does not present a problem when using a feature in the spectrum to determine the zero-point, since this method determines the undispersed position relative to the feature, both of which are shifted by the same amount.

Red-End Measurement

The final method is a variation on this last idea where the identifiable feature is created by the prism itself: the red end of the spectrum. Without any other filters in place, the prisms produce a spectrum where nearly all the light from 5000-6500Å fall within a couple of pixels, approximating a point source. This position can be measured in the image and the offset for 6000Å can be read from the dispersion curves. For example, for the NUV spectrum of Sand-3 described above, the red end of the spectrum was measured at Y=235. Assuming this corresponds to a wavelength around 6000Å, we find that this should correspond to an offset of 159, resulting in a calculated undispersed position of 235 + 159 or 391. The prime source of error in this method lies in the measurement of the end of the spectrum and in assigning a wavelength to it, and as we can see here we are only off by about 1 pixel in this example. However, if a filter was used in combination with the prism, it might cut off the observed spectrum at a wavelength other than 6000Å. This would make it difficult to know what the actual wavelength of the end of the spectrum really is, and therefore difficult to know what offset is associated with that end of the observed spectrum. In this case, a direct image at the same POS TARG would remove this ambiguity.

Photometry of the extracted spectrum

Photometric calibration of the spectrum requires knowledge of the percentage of observed light that was extracted from the spectrum. This is equivalent to knowing the encircled energy fraction for photometry of a point-source, only in this case it is an energy fraction of the extraction that is needed. This energy fraction was determined from background subtracted, single source images by dividing spectra of varying extraction widths by the spectra of a 140 pixel wide extraction. This provides some consistency with the DQE determinations for the FOC since the energy fraction of a point source has been defined to be 1.00 for an aperture with a radius of 70 pixels (see FOC-085 for more details). The energy fraction for a spectrum of a given extraction width was determined for each prism, with the results given in Table 2.

Table 2. Energy fractions for spectra as a function of the extraction width.

Extraction Width (pixels)	NUVOP	Error (3σ)	FUVOP	Error (3σ)
5	0.554	0.074	0.480	0.080
7	0.627	0.069	0.557	0.079
9	0.680	0.065	0.616	0.073
11	0.720	0.059	0.660	0.058

The energy fractions given in Table 2 are mean values based on measurements of the Sand-3 and HZ4 calibration observations. The 3s errors reflect the variations in the energy

fraction induced primarily by the effects of breathing and linearity in the spectrum and represent the range of variations that can be expected in well-exposed science observations.

The spectrum shown in Figure 3 was extracted with a 7 pixel wide aperture. Since this is a NUVOP spectrum, the encircled energy in this extraction is 0.627 based on Table 2. This will be the value used during the final calibration of the spectrum.

Calibration of the extracted spectrum

The IRAF task *objcalib* in the *hst_calib.foc.focprism* package handles the calibration of the extracted spectrum in one operation. It requires the input of the following information derived upon completing the steps in the previous sections:

- name of the extracted spectrum [*input*]
- position of the undispersed target [*yzero*]
- observation mode of the image [*obsmode*] (e.g. foc,f/96,prism2,f195w)
- exposure time of the image [*texp*]
- encircled energy (photometry) of the extracted spectrum [*encirc*]

The parameter names from the task are provided in brackets. The calibration of the spectrum shown in Figure 3 requires the input of the parameters in the task as follows:

```
      input = "nuv165b_ex7.ms" name of input spectrum file
     output = "nuv165b7_disp392" name of output resampled spectrum file
    obsmode = "foc,f/96,costar,prism2,f165w" observation mode
      yzero = 392.             Y pixel coordinate of undispersed image
    (wfirst = 1600.)          starting wavelength of resampled spectrum
     (wlast = 6000.)           last wavelength of resampled spectrum
        (dw = 1.)              bin width of resampled spectrum
(calibrate = yes)              correct the photometry as well as rebin?
      (texp = 895.75)          exposure time
    (encirc = 0.6274)          encircled energy fraction
      (n_wl = "c1")            column name for wavelength
    (n_flux = "c2")            column name for flux
(dispfiles = "")               pset for names of dispersion files
      (area = 45238.93416)     telescope area in cm^2
 (graphtab = "crcomp$hstgraph_*.tab") name of graph table
  (comptab = "crcomp$hstcomp_*.tab") name of components table
  (Version = "16March1994")  date of installation
      (mode = "al")
```

The parameters input into the task will calibrate the NUVOP+F165W spectrum of Sand-3 (`nuv165b_ex7.ms`) and create the wavelength and flux calibrated spectrum (`nuv165b7_disp392`). The starting wavelength of the calibrated spectrum (given as the parameter *wfirst*) should be 1600Å for NUV spectra and 1100Å for FUV spectra since those are the wavelength limits for the respective objective prisms.

This routine will apply the calibrated dispersion curve to the extracted spectrum; this spreads out the light from each pixel into equal wavelength bins. The throughputs of the filters and the FOC are then applied to the spectrum to convert them from counts sec^{-1} to ergs cm^{-2} sec^{-1} A^{-1} resulting in the calibrated spectrum, shown in Figure 4 for Sand-3.

Figure 4: Calibrated spectra of Sand-3. The comparison spectra (dotted) has been plotted to show the agreement. The region from 3200Å - 3900Å in the comparison spectrum denotes where the IUE spectra ends and the visible, ground-based spectra begins.

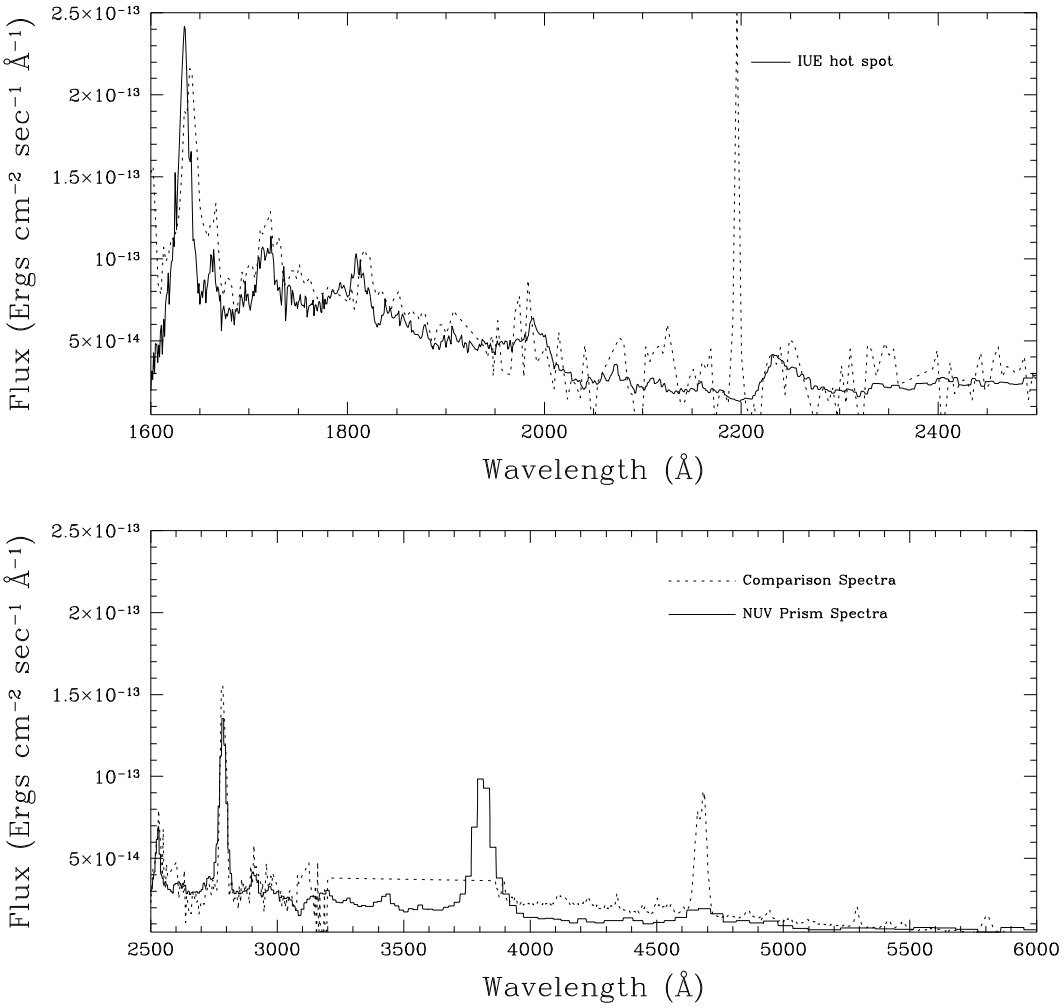

4. Calibration Results

The analysis procedure outlined here was applied to the observations of Sand-3 and HZ4 listed in Figure 1, starting with the initial dispersion curves that were part of the focprism package. The resulting spectra of Sand-3 was then compared to the comparison spectra, comprised of IUE and ground-based visible spectra, in an attempt to identify the observed lines. These lines were then identified in the objective prism spectra to determine their pixel position, and this was subtracted from the undispersed position to obtain the offset. The final determinations of the wavelengths and image positions are given in Table 3 for the NUVOP+F165W image of Sand-3 and in Table 4 for the FUVOP+F140W image of Sand-3.

Table 3. Emission line IDs from NUVOP+F165W Sand-3 image.

IUE λ(Å)	Fit λ(Å)[a]	Residual λ(Å)	Measured Y Position	Offset[b]	Fit Offset[c]	Residual Offset	Comments
1602.	N/A	N/A	955	-563	-568	5	Added as a boundary condition for short wavelength end of fit
1666	1663	3	868	-476	-480	4	
1710	1712	-2	804	-412	-410	-2	
1817	1807	10	690	-297	-291	-6	
1983	1986	-3	567	-175	-181	6	
2532	2527	5	393	-1	2	3	
2603	2602	1	379	13	14	-1	
2784	2782	2	354	38	40	-2	
2908	2902	6	340	52	54	-2	
2957	2968	-11	333	59	59	0.	
3811	3808	3	279	113	113	0	Wavelength estimated from paper on optical spectra
4343	4377	6	260	132	131	1	
6025	N/A	N/A	235	157	159	-2	Added as a boundary condition
6625	N/A	N/A	227	165	166	-1	Added as a boundary condition for long wavelength end of fit

a. This value refers to the wavelength of the feature as it appears in the calibrated NUVOP spectrum.
b. The Offset refers to the difference between the Measured Y position and the assumed undispersed position of the source, which is taken to be Y=392.
c. This offset refers to the position from the fit for the IUE λ.

Table 4. Emission line IDs from the FUVOP+F140W Sand-3 image.

IUE λ (Å)	Fit λ(Å)	Residual λ (Å)	Measured Y Position	Offset	Fit Offset	Residual Offset	Comments
1150	N/A	N/A	700	-449	N/A	N/A	Added as a boundary condition
1214.	N/A	N/A	(260)	-408	-408	0	Lyman a shadow of 0.8” occulting finger
1241.25	1238	3	646	-395	-394	-1	
1374.03	1379	-5	595	-344	-346	2	
1551.94	1547	5	564	-313	-312	-1	
1642.23	1632	10	553	-302	-302	0	
2223.	2229	-6	523	-272	-272	0	
2531.86	2481	51	514	-263	-264	1	
2783.97	2775	8.	512	-261	-260	-1	
4000	N/A	N/A	(104)	-252	-251	-1	Zodiacal light shadow of 0.8” finger
6600	N/A	N/A	499	-248	N/A	N/A	Added as a boundary condition

Fitting method

The offsets given in the tables were then fit to the inverse of the wavelengths using the task *gfit1d* to obtain a dispersion curve for each prism. High order models provided lower residuals, however, the complex fits dramatically altered the photometry in those regions where the dispersion curve changed the most; therefore, the dispersion curves were both fit using a simple 2nd order spline model. The wavelengths listed at the long and short wavelength ends of each spectra were added as a boundary condition for the fit to better match the wavelengths at the ends where either the lines are too faint or the wavelength dispersion is too steep.

NUVOP Dispersion Curve

The derived dispersion curve was then applied to the HZ4 data in order to see if the known spectrophotometry could be recovered from the NUV objective prism spectrum. Initial fits showed some significant discrepancies which were used to eliminate errors in the fit and with iteration between the HZ4 data and the Sand-3 data a final fit was determined. This dispersion curve adequately reproduced the HZ4 spectral shape over most of the wavelength range, as can be seen in Figure 5. The disparity in the flux from 1600-1800Å may be due to reduced transmission in the NUV prism relative to the expected throughput. This should be taken into account when performing spectrophotometry in that wavelength range with the NUV prism.

FUVOP Dispersion Curve

The FUVOP dispersion curve was derived using the same method of fitting the wavelengths of Sand-3 emission lines and iterating with the photometry of HZ4 as done with the NUVOP data. In addition to the lines seen in Sand-3, the observed separation between the Lyman α shadow and the zodiacal light shadow of the 0.8” occulting finger in images taken by P. Jakobsen provided unambiguous wavelengths and positions for the fit. The observed positions of the two finger shadows were subtracted from the POS TARG used for the observation in order to obtain the dispersion offsets for each position(wavelength). The wavelength for the zodiacal light shadow corresponded to the peak wavelength in the zodiacal light spectrum multiplied by the FOC+OTA DQE; this resulted in a wavelength of 4000Å as determined from FOCSIM. These values were then used to fix the ends of the FUVOP dispersion in the fit. P. Jakobsen graciously provided the checks on the derived FUVOP dispersion curve using his own data, further insuring its accuracy.The final dispersion curve derived for the FUVOP was then applied to FUVOP observations of HZ4, as shown in Figure 6.

Figure 5: Photometric calibration of the NUVOP. This plot compares the NUVOP spectrum of HZ4 (**solid**) with the comparison spectrum from the calibration library(**dotted**).

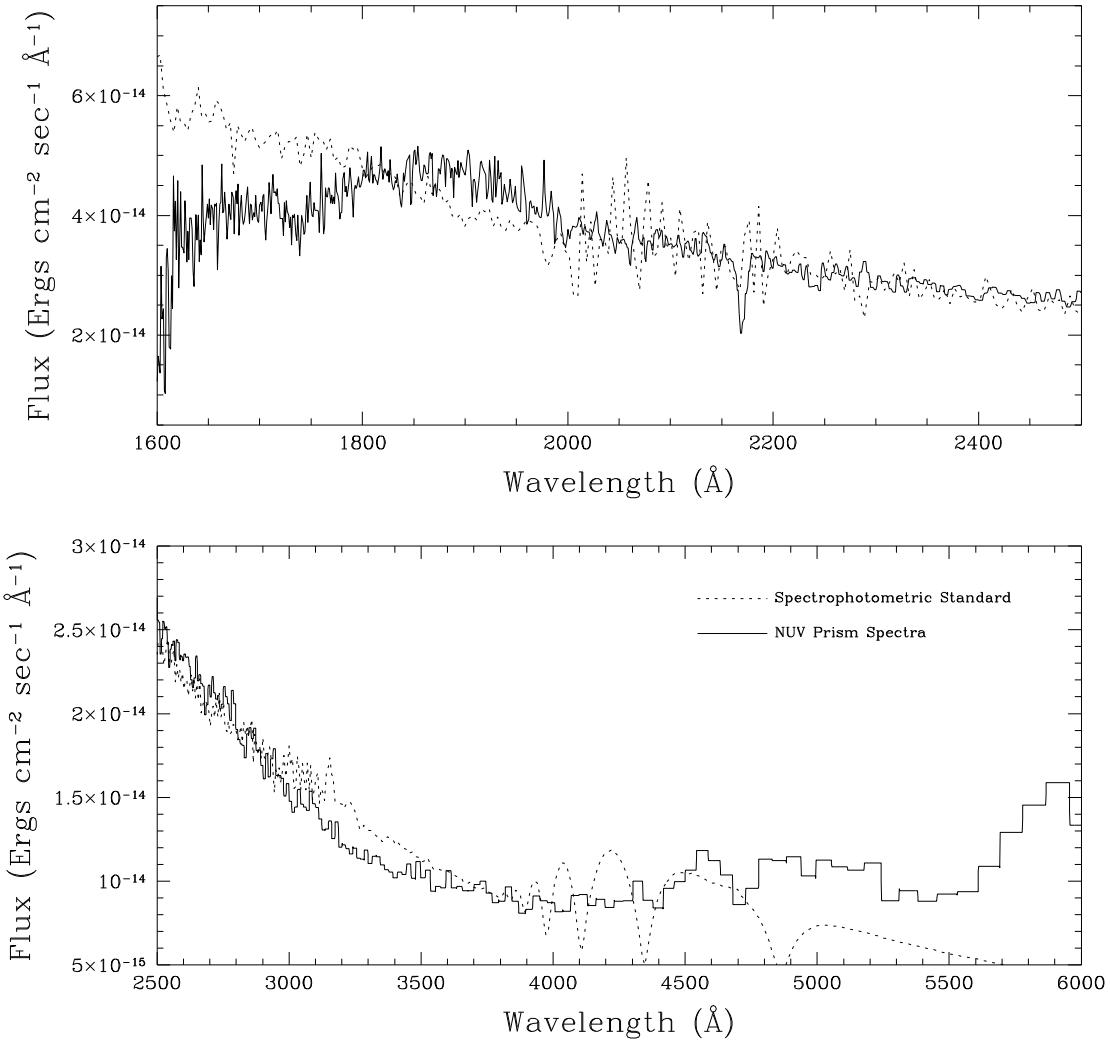

Errors in the calibrations

The final dispersion curves, shown in Table 5, had rms errors in the fit of 0.86 pixels for the FUVOP dispersion curve and 3.43 pixels for the NUVOP dispersion curve, as can be seen in Table 3 and Table 4. These errors translate to 4Å at 1600Å and 60Å at 3500Å for the NUVOP and 1.3Å at 1150Å and 22Å at 2000Å for the FUVOP. This can be seen in Table 3 and Table 4 by comparing the IUE wavelength assigned to the features with the wavelength derived from the fit for each prism. The *synphot* package was also used to calculate the apparent magnitudes for different passbands (F190M, F220W, F278M, U, B, and V) using both the calibrated spectra and the spectrum from the calibration spectra library. These calculations indicate that the photometry for HZ4 with the NUVOP was

Figure 6: Calibration of Far-UV Objective Prism spectrum of HZ4.

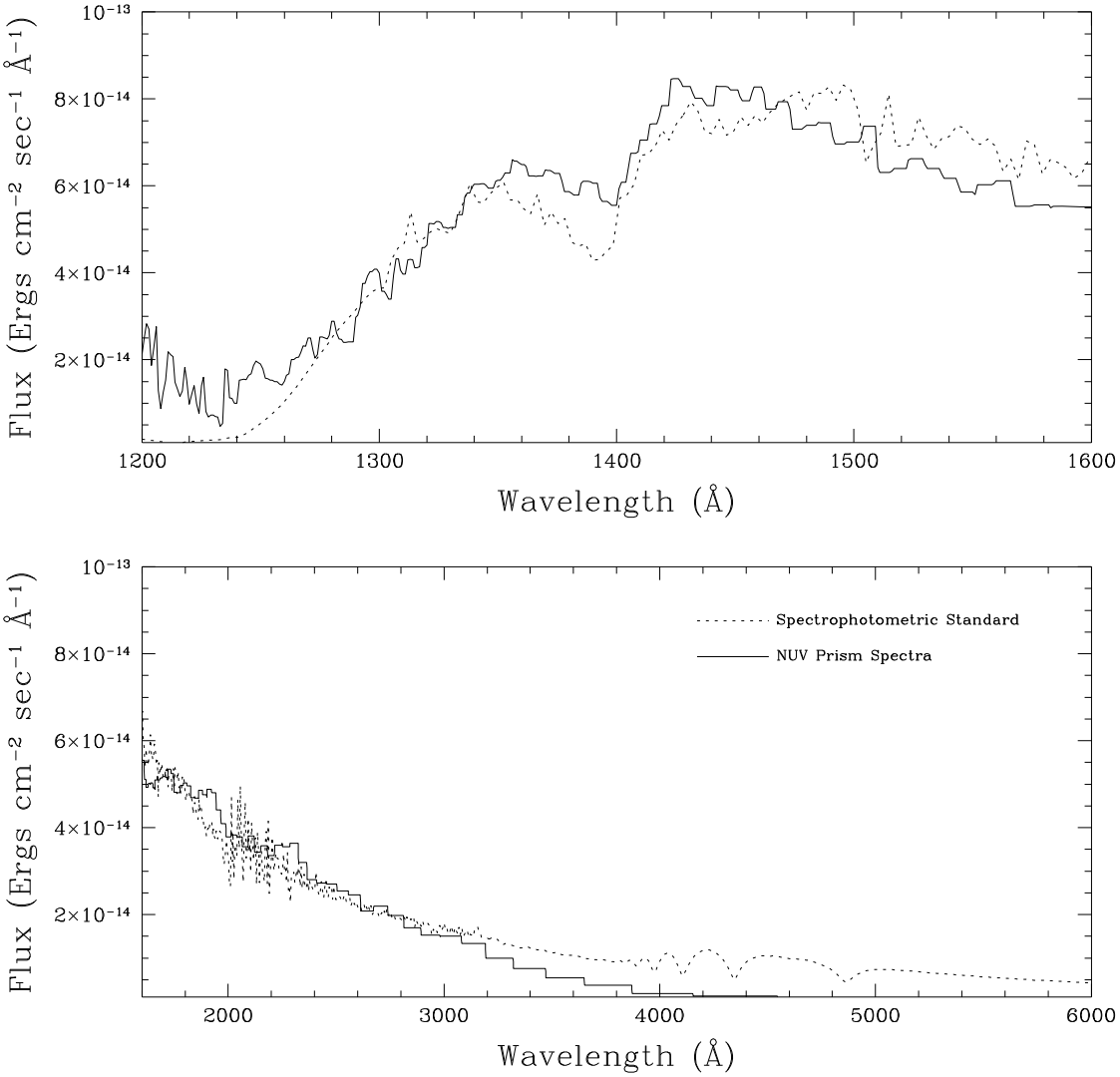

within 0.1 magnitudes from 1600Å - 4000Å and 0.4 magnitudes from 4000-6000Å, while the FUVOP spectrum was within 0.1 magnitudes of the catalog spectrum between 1240Å to 3000Å. Similar results were obtained for the Sand-3 data as well, although it is not an established photometric standard so the agreement can not be taken by itself as an indication of the accuracy of the calibrations.

5. Conclusions

New dispersion curves were derived for both the far-UV (FUVOP) and near-UV (NUVOP) objective prisms and are presented in Table 5. The dispersion curves provide the relation between a feature's position in the image to a wavelength, however, the wavelength range covered in a pixel determines how the observed counts are distributed across the wavelength range spanned by each pixel. Both relations, the dispersion curve and the

dλ/dx relation, are shown in Figure 7. The NUVOP curve derived here represents a tremendous improvement over previous versions, providing for the first time reduction of NUVOP spectrum with errors of known accuracy, with photometric accuracy within 0.1 mag from 1800-4000Å. The FUVOP dispersion curve also improved with the latest calibrations, allowing for photometric errors around 0.1 mag from 1300-3000Å. The regions of highest photometric accuracy overlap enough to allow complete spectral coverage with generally 0.1 mag errors from 1300-4000Å from just two images, a significant capability onboard HST.

In addition to the new dispersion curves, the techniques for reducing objective prism data was refined and explained for general application to all prism data. As a result, observers have the necessary tools to reduce objective prism data and rigorously tested calibrations to apply with errors in line with general photometry available with any FOC data.

Figure 7: (a) Dispersion curve and **(b)** dλ/dx relation for the NUV objective prisms, and **(c)** dispersion curve and **(d)** dλ/dx relation for FUV objective prisms.

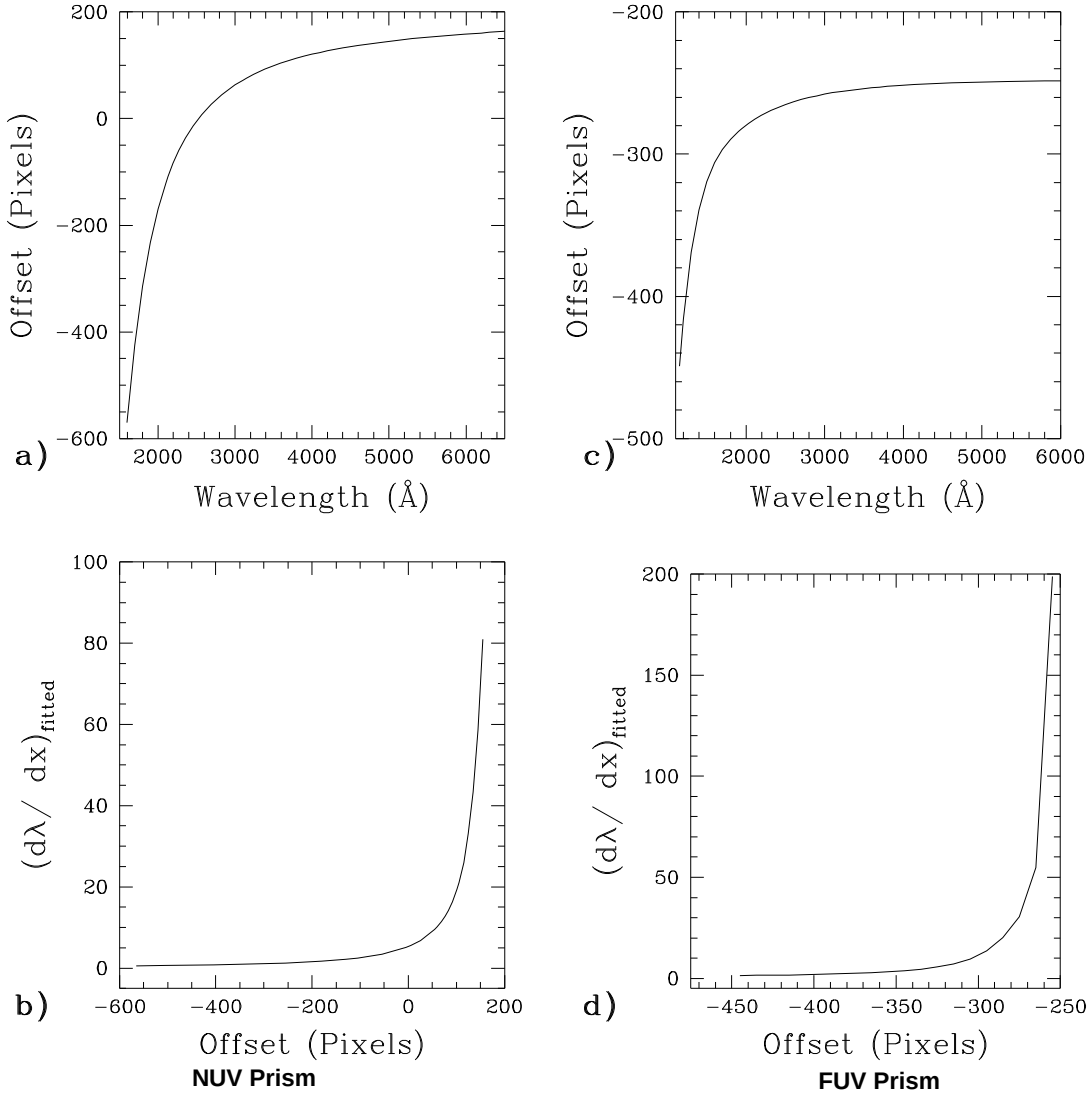

Table 5. Dispersion curves for the F/96 NUVOP and FUVOP

NUVOP		FUVOP	
Wavelength (Å)	**Offset**	**Wavelength(Å)**	**Offset**
1600.	-570.48	1150.	-449.18
1700.	-424.60	1200.	-416.01
1800.	-315.01	1300.	-369.13
1900.	-232.39	1400.	-339.20
2000.	-173.15	1500.	-319.50
2100.	-122.05	1600.	-306.10
2200.	-82.91	1700.	-296.60
2300.	-52.70	1800.	-289.56
2400.	-27.57	1900.	-284.07
2500.	-6.31	2000.	-279.56
2600.	11.67	2500.	-265.08
2800.	40.44	3000.	-257.81
3000.	62.43	4000.	-251.51
3500.	99.03	5000.	-249.25
4000.	120.96	6000.	-248.40
4500.	135.32	6600.	-247.97
5000.	145.38		
5500.	152.81		
6000.	158.54		
6600.	165.58		